JJEE
Volume 11 | Number 4 | Pages 705-719

Jordan Journal of Electrical Engineering

ISSN (print): 2409-9600, ISSN (online): 2409-9619

Homepage: jjee.ttu.edu.jo

Experimental Characterization of Conducted EMI in DC/DC Buck Converters: Effects of Duty Cycle and Switching Device

Abdeslam Lahmani[1*], Houcine Miloudi[2], Sami Mohammed Bennihi[3], Mohammed Hamza Bermaki[4], Mohamed Miloudi[5], Abdelkader Gourbi[6], Abdelber Bendaoud[7]

[1, 2, 4, 5, 7] APELEC Laboratory, Faculty of Electrical Engineering, University of Djilali Liabes, Sidi Bel Abbes, Algeria
E-mail: abdeslam.lahmani@univ-sba.dz
[3] Faculty of Electrical Engineering, University of Djillali Liabes, Sidi Bel Abbes, Algeria
[5] Electrical Engineering and Automation Department, Ahmed Zabana University, Relizane, Algeria
[6] Institute of Science and Applied Techniques, Ahmed Ben Bella University, Oran, Algeria

Received: Sep 11, 2025 *Revised: Nov 21, 2025* *Accepted: Dec 03, 2025* *Available online: Jan 20, 2026*

***Abstract*—** The electromagnetic interference (EMI) conducted by a DC/DC buck converter was experimentally investigated in this study. The research focused on the influence of the duty cycle and the selection of switching devices—metal-oxide-semiconductor field-effect transistor (MOSFET) or insulated-gate bipolar transistor (IGBT)—on both common-mode (CM) and differential-mode (DM) emissions. Measurements were conducted in accordance with the EN 55022 conducted emission standard, covering the frequency range from 150 kHz to 30 MHz, using a Line Impedance Stabilization Network (LISN) and a spectrum analyzer. The results reveal that DM emissions dominate the conducted spectrum, exceeding the Class B limit in a narrow frequency band at lower frequencies, while CM emissions generally remain within the limits across most of the measured range. Overall, lower duty cycles lead to higher CM and DM emission levels, whereas higher duty cycles result in a significant reduction in total noise. A comparison of the switching devices shows that the MOSFET-based converter generates more CM noise due to its rapid switching, while the IGBT-based converter maintains lower CM noise but exhibits slightly higher DM emissions under certain conditions. In conclusion, the converter is close to meeting EN 55022 Class B standard and requires only minor adjustments at low frequencies to achieve full compliance. These findings provide valuable insights into the impact of control parameters and semiconductor selection on conducted EMI, contributing to the design of DC/DC converters that are both efficient and compliant with electromagnetic compatibility (EMC) regulations.

***Keywords*—** Chopper; Conducted EMI; Common mode; Differential mode.

1. INTRODUCTION

Recent advances in power electronics have intensified the need for accurate characterization of conducted electromagnetic interference (EMI) in various electrical systems. Several studies have shown that both common-mode (CM) and differential-mode (DM) disturbances remain critical in applications such as variable-speed motor drives, switch-mode power supplies, and induction motor feeders [1–3]. These investigations highlight how switching devices, parasitic paths, and converter topologies strongly influence disturbance propagation. In particular, the experimental assessment of EMI behavior has become essential for understanding noise mechanisms and guiding the design of compliant and efficient power converters. Parallel research efforts have focused on improving electromagnetic compatibility (EMC) through optimized filtering, shielding, and converter parameter selection. Work on

* Corresponding author
DOI: https://doi.org/10.5455/jjee.204-1757601934

EMC filters in variable-speed systems, the effectiveness of magnetic shielding, and the behavior of hybrid photovoltaic supply systems all demonstrates that EMI mitigation depends simultaneously on converter architecture and operating conditions [4–6]. Further contributions examining EMI in chopper-based drives, radiated noise from power converters, and DM impedance in induction motors reinforce the importance of detailed experimental analysis to ensure compliance with EMC standards while maintaining energy-conversion performance [7–9]. These findings collectively underline the necessity of systematic EMI evaluation in modern DC/DC converter design.

The buck converter is a step-down DC/DC converter that is ubiquitous in its application converting a higher input voltage into a lower output voltage. It is an essential and fundamental circuit in power electronics today, and its applications are not limited to but include switch-mode power supplies (SMPS), smartphones, laptops, battery chargers, and green energy [10–12]. The operation of these converters is made possible by fast-switching semiconductor devices, mainly MOSFETs and IGBTs, which lead to voltage (dv/dt) and current (di/dt) transitions being very sharp. Though it is a big advantage to be able to switch faster for improved efficiency and smaller sizes, it however leads to a great amount of EMI [13–16]. EMI can be transmitted either by conduction through the wires the EMI is along (conducted EMI) or through space by the electromagnetic fields (radiated EMI) [17, 18]. Conducted EMI is further categorized into two modes: DM and CM. In DM, the converter applies a pulse-width modulated (PWM) voltage between phases leading to currents flowing through the conductors in opposite directions [19–21]. CM is the case which would cause the parasitic currents to flow in the same direction along all the conductors and to ground through parasitic capacitances and CM impedances.

The demand for higher power density and switching frequency has led to increased EMI concerns, not only in traditional silicon devices (MOSFETs and IGBTs) but also in the new wide-bandgap technologies including Gallium Nitride (GaN), and Silicon Carbide (SiC) MOSFETs [22]. This development necessitates a very careful converter design, extensive EMI filtering, and detailed experimental characterization to comply with strict EMC standards, which often have increasingly narrow compliance margins. EMI modeling and predicting can be done either in the time or frequency domain [23-25]. The time-domain methods use circuit simulation software like SPICE to simulate the operation of the converter, with the EMI spectrum being extracted via Fast Fourier Transform (FFT). On the other hand, frequency-domain methods rely on either analytical model for estimating the EMI spectrum or direct experimental measurement [26, 27].

Recent research [28-30] have focused on EMI modeling, forecasting and filter design techniques for EMI, resulting in improvements in the EMC of power converters. However, the noise characteristics of CM and DM converters under the same experimental conditions have only been examined by a limited number of studies regarding the simultaneous effects of duty cycle variation and switching device type. This research aims to address this issue by offering a fresh experimental perspective: (1) the impact of duty cycle variation on CM and DM emissions of a MOSFET-based chopper converter and (2) a comparative evaluation of the EMI trend between MOSFET and IGBT devices under the same functional parameters.

The dual approach provides practical insight into the differences in EMI performance between these two semiconductor technologies and evaluates their compatibility with EN55022 Class B conducted emission limits. The results enhance our understanding of the

interplay between switching device choice and control parameters in DC-DC converter EMI generation mechanisms. Table 1 provides a summary of various studies concerning electromagnetic interference (EMI) in different power converter topologies. The papers included in the review primarily focus on conducted EMI, particularly in the areas of chopper converters and rectifiers, where indirect prediction techniques, along with experimental measurements, have become standard practice. A small number of studies have developed prototypes, suggesting that most research is still in the modeling phase. Radiated EMI studies are less common, with subjects mainly focusing on non-isolated and flyback converters. Researchers in this area conduct direct experimental measurements and advocate for EMI mitigation through printed circuit board (PCB) layout optimization, cross-capacitor techniques, and the use of common-mode chokes.

Table 1. EMI DC/DC converters in literature.

Converter type	Fabricated	Predicted EMI	Method of prediction	Mitigation method	Parameters investigated
Flyback converter [16]	*	radiated	Direct Experimental Measurement	*	CM choke impedance
Isolated full bridge [31]	*	conducted	Indirect Experimental Measurement	HF Filter	NA
Rectifier [32]	✓	conducted	Indirect Experimental Measurement	*	NA
Chopper Serie [33]	✓	conducted	Indirect Experimental Measurement	*	NA
Chopper Serie [34]	*	conducted	Indirect Experimental Measurement	*	Mosfet, IGBT
Boost converter [35]	*	conducted	Experimental Measurement	Filter	*
Non isolated Power converter [36]	*	radiated	Direct Experimental Measurement	Optimizing pcb layout Cross capacitor	*
Chopper Serie [37]	*	conducted	Indirect	*	α,tm,f,td

In general, the papers emphasize high-frequency (HF) filtering and layout improvements as the main strategies for reducing EMI, while the selection of devices, such as the choice between MOSFETs and IGBTs, remains a significant factor. Duty cycle, switching frequency, dead time, and switching device type are the primary parameters under examination, as they all strongly influence EMI generation. Overall, current literature indicates that conducted EMI is still the dominant issue, with very few comprehensive methods that simultaneously address both prediction and mitigation. The challenge of developing design strategies that optimize performance while ensuring compatibility with electromagnetic interference continues to require further research.

2. MATERIALS AND METHODS

This section outlines the necessary steps for designing and implementing the buck-type DC/DC converter, also referred to as a series chopper, for the EMC test bench setup used in experimental measurements. The chopper functions as a converter, transforming a fixed direct current (DC) input voltage or current into a variable continuous output at a different level using pulse-width modulation This type of converter is widely used in power electronics for several reasons, primarily its efficiency, HF switching capability, and simplicity. Figure 1 illustrates the general topology of the converter, which consists of a switch, a diode, an inductor, and a load resistor (Fig. 1).

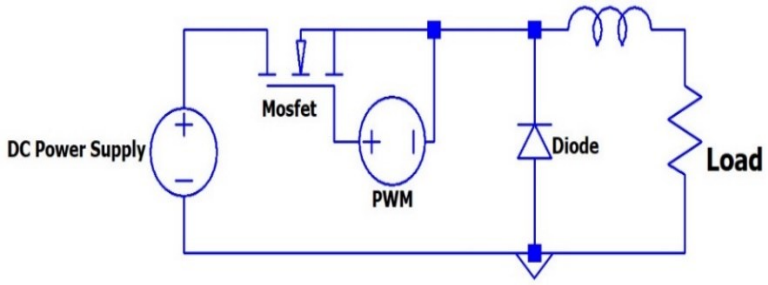

Fig. 1. General configuration of the buck converter.

The circuit consists of a standard N-channel enhancement-mode MOSFET (IRF840) used as the main switching device (on/off). When the MOSFET is turned off, a fast recovery diode (BYT12P600) is employed to provide a freewheeling path for the inductor current. A purely resistive load of 1 kΩ is connected to the output of the chopper. MOSFET control is achieved through a PWM signal generated by a PIC 16F877A microcontroller operating at 5 volts. A gate driver (IR2110) is dedicated to translating and amplifying the control signal, as the MOSFET requires a higher gate voltage and cannot be directly driven by the microcontroller.

The two push-buttons responsible for the control logic can be manually used to adjust the duty cycle: one increases the duty cycle (α), while the other decreases it. This control method allows for the study of the effect of varying the PWM on the chopper's performance, including its EMI behavior under different operating conditions. The microcontroller and gate driver circuit are powered by steady 5V and 12V supplies, respectively, from voltage regulators. A 20V DC input powers the chopper, and the output voltage is monitored to ensure proper operation and response to duty cycle modulation. The assembled hardware, shown in Fig. 2, is mounted on a printed circuit board, with careful attention paid to trace layout and grounding to minimize radiated EMI and parasitic inductance.

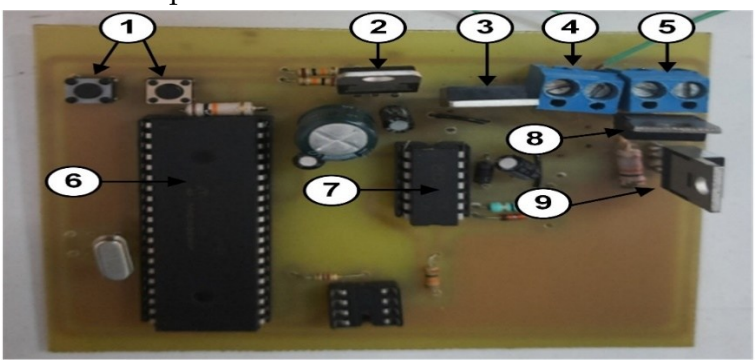

Fig. 2. PCB layout of the implemented chopper circuit. 1) Push-buttons; 2) 5 V regulator; 3) 12 V regulator; 4) Load terminals; 5) Power supply input; 6) PIC16F877A microcontroller; 7) IR2110 gate driver; 8) BYT12P600 diode; 9) IRF840 MOSFET.

Figure 3 shows the proper output voltage waveform of the chopper, confirming correct operation. As expected, the average output voltage varies linearly with the duty cycle of the PWM signal. The significance of these characteristics lies in their ability to parametrically examine the relationship between switching control and EMI emissions.

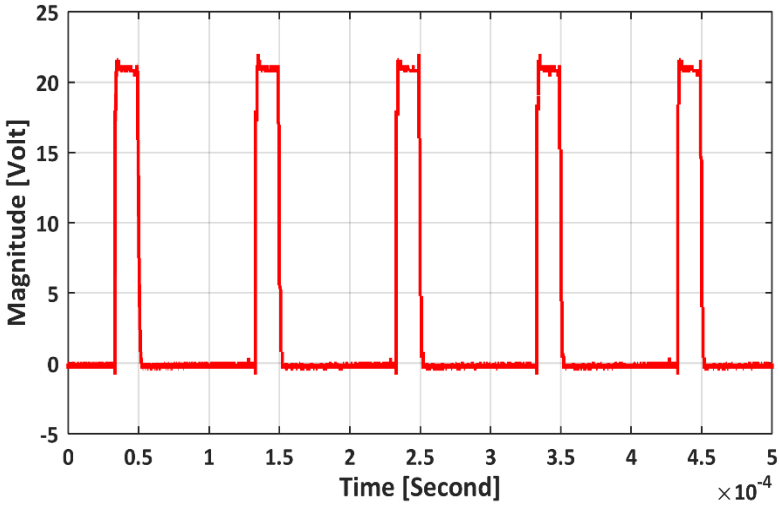

Fig. 3. Temporal variation of the chopper output voltage.

To quantify the conducted EMI generated by the converter, current measurements for both CM and DM noise were taken (Fig. 4). These types of conducted noise have distinct propagation paths and physical sources. The intended current path, modulated by HF switching transients represented by the DM currents, flows in opposite directions through the phase conductors and returns to the neutral line. In contrast, CM currents flow in the same direction through the conductors with respect to the ground before returning to the environment via parasitic paths, such as stray capacitances (Fig. 5).

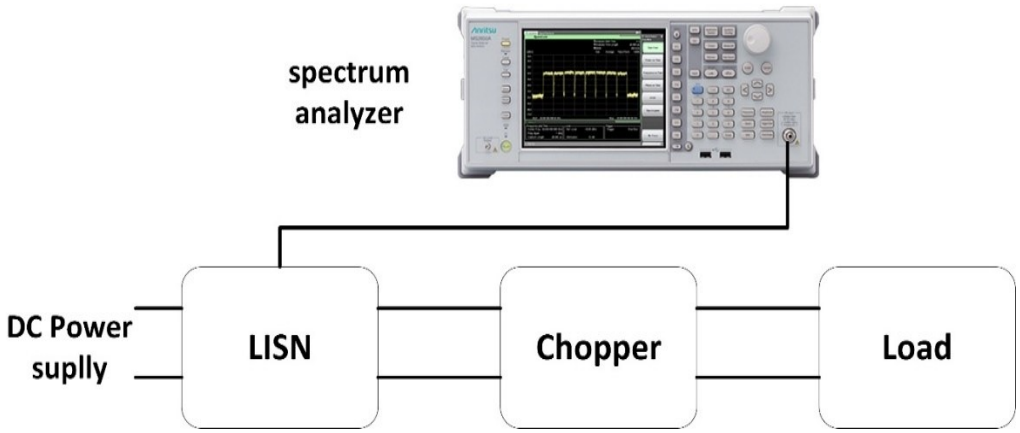

Fig. 4. Diagram of the EMI measurement setup according to EN55022.

To differentiate between the CM and DM currents, two different probe configurations were used with a high-bandwidth current probe, as illustrated in Fig. 6. For CM measurements, both the supply and return conductors are looped through the probe in the same direction. For DM measurements, the current probe is wrapped around a single conductor, either positive or negative. This configuration allows for the isolation of the components of the conducted electromagnetic spectrum and facilitates an exploration of their relationship with switching device type and duty cycle variation.

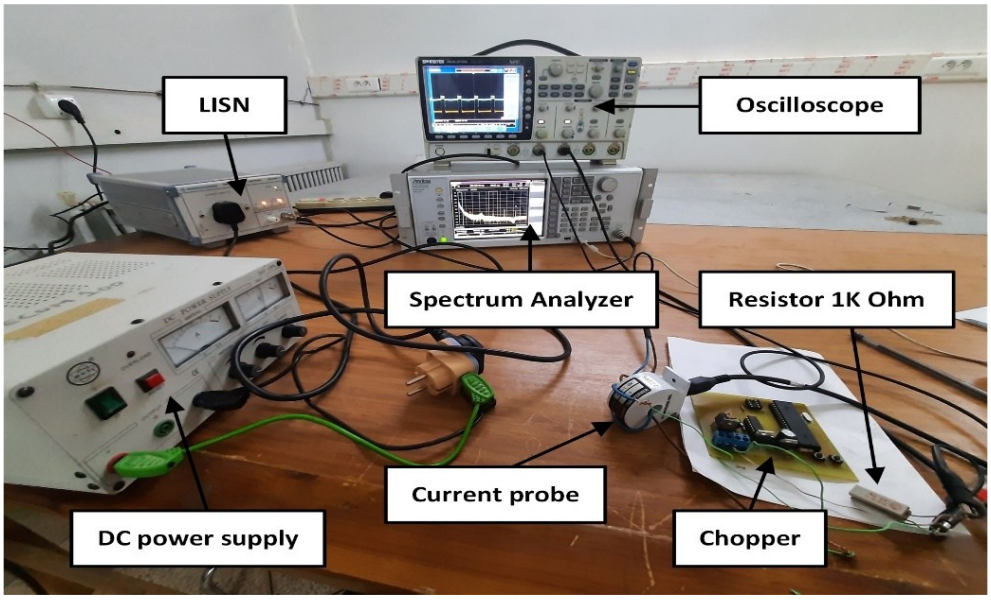

Fig. 5. Photograph of the experimental EMI measurement bench.

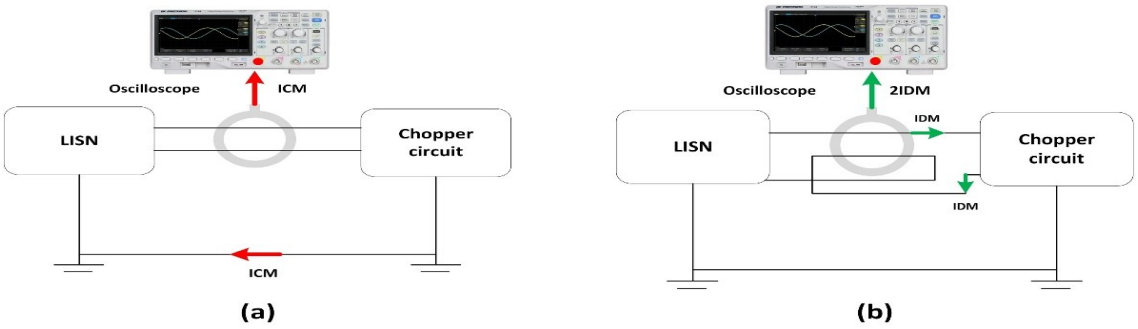

Fig. 6. Current probe configurations for measuring (a) CM and (b) DM noise.

According to the EN55022 standard, there are two categories of conducted emission limits for electronic equipment. The first category, "Class A," is intended for use in industrial environments, while the second, "Class B," is designed for residential, commercial, or medical facilities. This standard sets limits for conducted emissions across specified frequency bands, using both quasi-peak and average detector readings measured in dBµV. The limits for Class B are stricter, reflecting the greater sensitivity of residential environments to EMI [8]. The thresholds of the limits are displayed in Fig. 7, according to the EN55022 standard, for both Class A and Class B. Further details are provided in Table 2, which showcases the limits. The objective of these measurements is to verify whether the emissions of the converters remain within the specified limits across a range of duty cycles and switching conditions.

This can be achieved by comparing the measured EMI data to the defined limits, enabling an assessment of whether the converter's design complies with the regulations. Additionally, this comparison helps identify critical operating conditions or frequencies that may cause emissions to exceed acceptable levels.

3. RESULTS AND DISCUSSION

The propagation mode of the conducted electromagnetic disturbances generated by the chopper was the first parameter investigated in this study. This is a crucial part of the work, as

it provides insight into the disturbance levels that contribute more significantly to EMI through CM and DM modes, since they differ in coupling mechanisms and mitigation requirements.

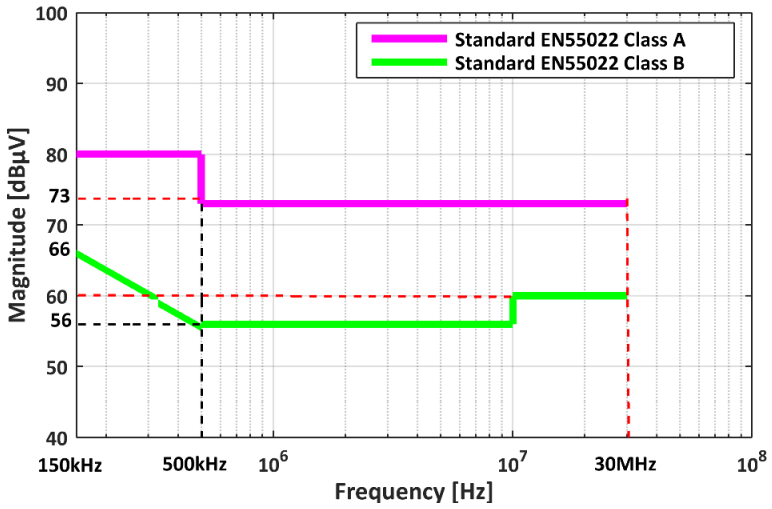

Fig. 7. EN55022 Class A and B conducted emission limits [7, 22].

Table 2. EN55022 standard limits values [23].

	EN55022 class A conducted EMI limit		EN55022 class B conducted EMI limit	
Frequency range [MHz]	Quasi-Peak	Average	Quasi-Peak	Average
0.15 to 0.50	80	66	66 to 56	56 to 46
0.5 to 10	73	60	56	46
5 to 30	73	60	60	50

The temporal waveforms and frequency spectrums for both CM and DM noise currents are shown in Figs. 8 and 9, respectively. It was observed that, across the entire frequency measurement range, DM exhibited higher amplitude levels compared to CM disturbances. This indicates that the chopper generates significantly more interference in differential mode, suggesting that EMC mitigation methods should focus more on DM noise suppression. This observation aligns with previous findings and general understanding, where CM noise is typically driven by capacitive coupling paths, while DM noise is associated with switching loops.

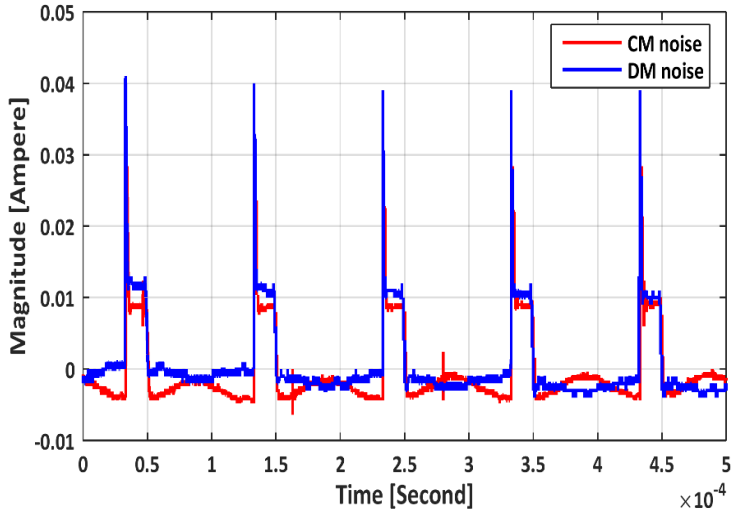

Fig. 8. Temporal variation of CM and DM measured currents.

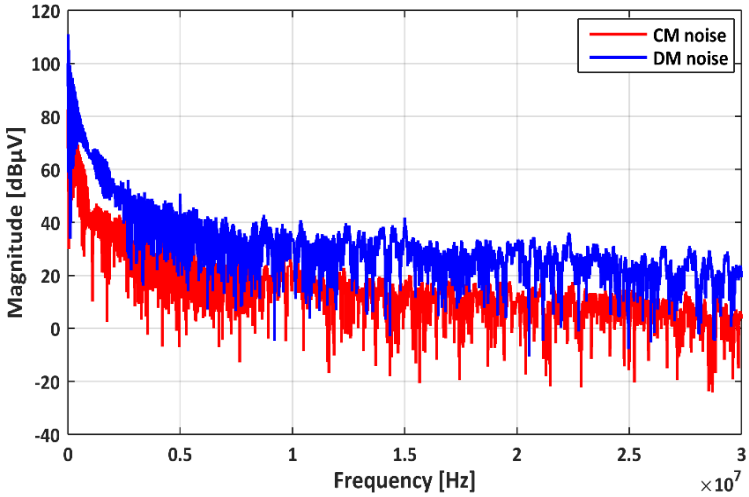

Fig. 9. CM and DM noises spectrum.

The primary source of EMI produced by static converters is the extremely fast switching transitions of semiconductor devices. The duty cycle of the PWM control signal determines these switching transitions and is typically chosen to optimize the converter's performance. However, the impact of the duty cycle on EMC behavior is often overlooked. To assess this effect quantitatively, an EMI test was conducted with two different duty cycles: a low duty cycle (α = 15%) and a high duty cycle (α = 90%).

In the CM spectrum shown in Fig. 10, it is clearly evident that lower duty cycles result in significantly higher emission amplitudes. At 10 MHz, the CM noise was approximately 30 dBµV at α = 15% and 20 dBµV at α = 90%, representing a reduction of about 33% at higher duty cycles. At 20 MHz, the CM noise was reduced from 15 dBµV (90%) to 5 dBµV (15%), corresponding to a 66% reduction. At 25 MHz, similar values were obtained: 15 dBµV at α = 15% and 5 dBµV at α = 90%, again confirming a ≈66% reduction at higher duty cycles. At 30 MHz, the CM noise dropped from 5 dBµV (α = 15%) to –5 dBµV (α = 90%), a difference of 10 dBµV (≈100% reduction relative to the 15% case.

The quantitative results demonstrate that the entire HF range (10–30 MHz) shows a considerable increase in the CM noise that is caused by lower duty cycles. This tendency is in line with the production of stronger HF components through shorter conduction intervals and faster dv/dt transitions at low duty cycles.

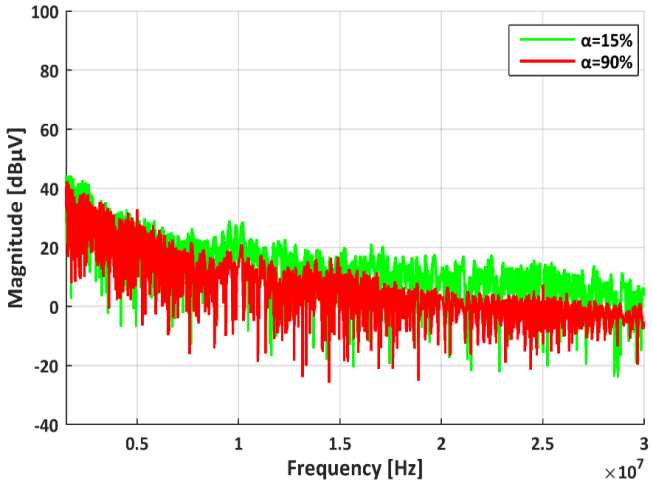

Fig. 10. CM current spectrum for α = 15% and α = 90%.

A similar trend is observed in the DM spectrum, as shown in Fig. 11. DM emissions exhibit a similar pattern to CM emissions, but with a less pronounced effect. In the region of the fundamental switching frequency (approximately 150 kHz), the DM noise levels were around 65 dBµV for α = 15% and 60dBµV for α = 90%, indicating an increase of nearly 8%. It was noticed that the DM noise level at 8MHz varied with the duty cycle. The overall DM noise measured approximately 40 dBµV at the 15% duty cycle and slightly reduced to around 37 dBµV at the 90% duty cycle. The DM noise level at 13 MHz and a = 15% was 35 dBµV, while for a = 90% it was 30 dBµV. The noise at 19 MHz dropped from 25 dBµV (a = 15%) to 20 dBµV (a = 90%). At 28 MHz the DM noise level was 28 dBµV for a = 15% and reduced to 19 dBµV for a = 90%.

The findings reveal the fact that the amplitude of DM noise is reduced as duty cycle increases, and at the same time, the overall frequency components are not significantly altered.

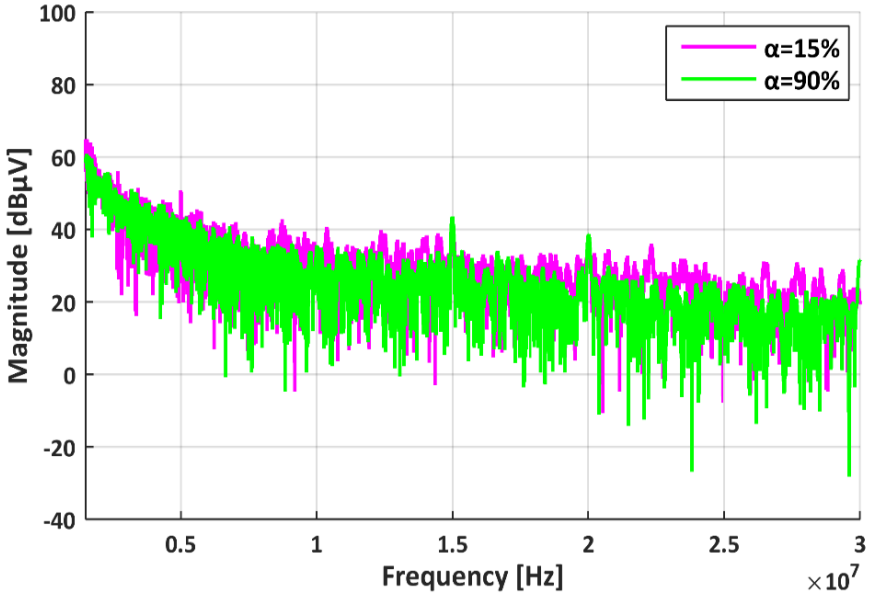

Fig. 11. DM noise specter with α =15%, α=90%.

The impact of duty cycle variation on the EMI spectrum was analyzed for MOSFET - based converters. The frequency position of the dominant harmonics remains determined by the converter's fixed switching frequency even if the duty cycle is changed, as revealed in the results. Instead, the variation in duty cycle primarily influences the amplitude of the conducted EMI. As the duty cycle increases, the pulse width modulation changes the energy distribution within each switching period, leading to noticeable differences in the magnitude of the emissions. As illustrated in Fig. 10, the CM noise amplitude decreases with higher duty cycles, while the DM emissions shown in Fig. 11 exhibit a similar but less pronounced variation.

Following the analysis of the propagation mode and duty cycle effects on the chopper's conducted disturbances, we focused on comparing the conducted EMI efficiency of two different switching devices: the C07JTG60N60 IGBT and the IRF840 MOSFET.

The CM and DM spectrum are illustrated and compared under the same operating conditions for both devices in Figs. 12 and 13, respectively. The comparison of the conducted EMI levels confirms the differences observed between the two switching devices. At 150 kHz, the DM noise measured approximately 74 dBµV for the MOSFET and 68 dBµV for the IGBT, indicating an increase of nearly 9% for the MOSFET. At 1 MHz, the CM noise reached about 66

dBµV for the MOSFET and 57 dBµV for the IGBT, corresponding to a 16% difference. At 10 MHz, both devices exhibited lower emission amplitudes due to the attenuation of parasitic elements at high frequencies; however, the MOSFET still produced emissions approximately 10% higher than the IGBT.

These results quantitatively confirm that the MOSFET generates stronger conducted noise, particularly in the HF range, due to its faster switching transitions and higher dv/dt. The IGBT, with its slower switching characteristics, maintains lower CM levels, offering a performance advantage in EMI-sensitive applications despite a slight compromise in switching speed and efficiency.

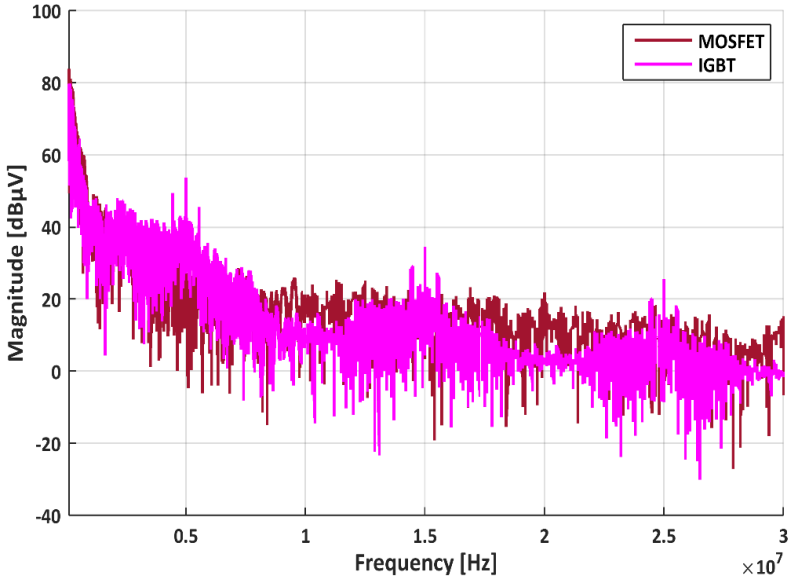

Fig. 12. Comparison of CM spectra for IRF840 and IGBT C07JTG60N60.

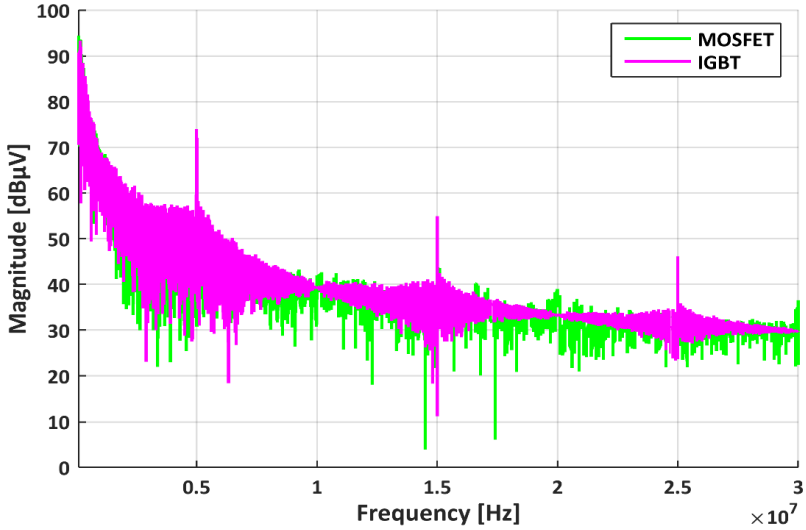

Fig. 13. Comparison of the DM spectra for IRF840 and IGBT C0TjTG60N60.

Since the commercialization of electronic power devices must comply with EMC standards, the final aspect of this study involved measuring the CM and DM spectrum to ensure compliance with the EN55022 standard, where emissions must remain within acceptable bounds. The CM noise, as illustrated in Fig. 14, generated by the chopper exceeds the EN55022 Class B limit in the 0.15–0.75 MHz frequency range. However, the results show

that the chopper remains compliant with the standard in the 0.75–30 MHz range. However, the DM noise, shown in Fig. 15, surpasses the EN55022 Class B limit between 0.15 and 2.5 MHz but remains below the limit for the remainder of the frequency range (2.5–30 MHz).

Overall, the results are favorable concerning CM emissions, as they mostly meet the established standard requirements. However, for DM emissions (Fig. 15), it is recommended to implement minor adjustments at the lower end of the spectrum. These may include duty cycle modifications, filter design optimizations, and gate resistance adjustments to ensure the entire frequency band is addressed effectively without compromising the converter's efficiency.

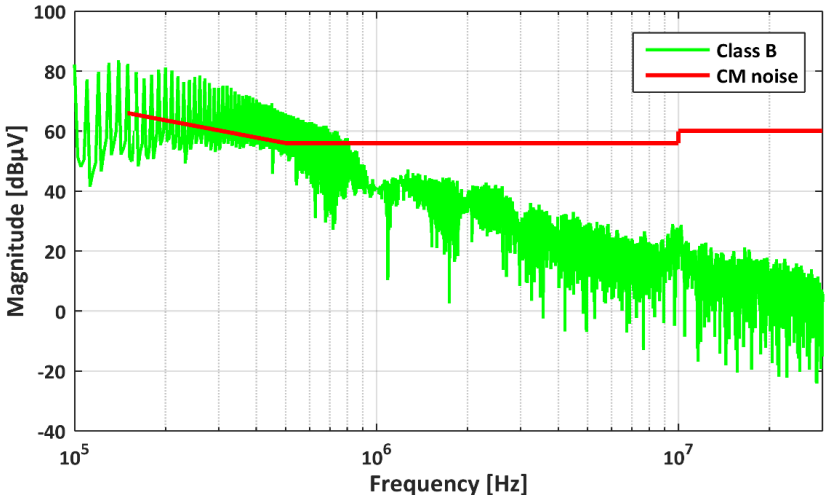

Fig. 14. CM noise spectrum compared with the EN55022 limit Class B.

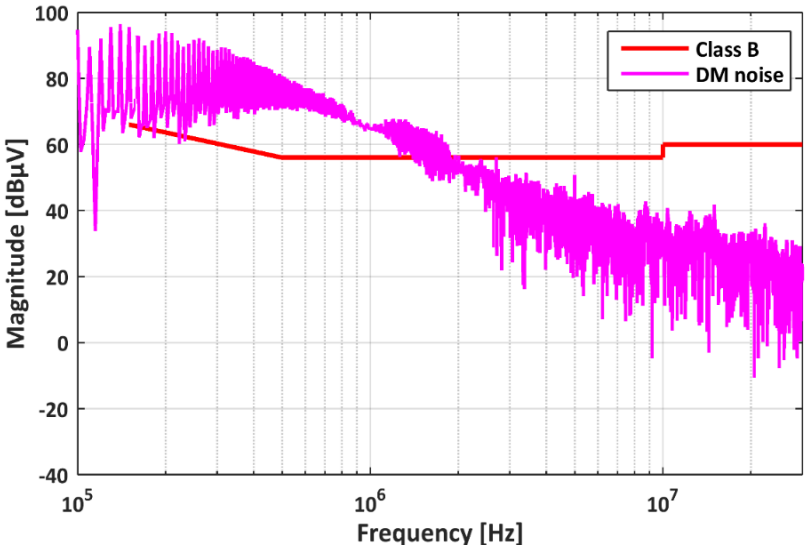

Fig. 15. DM noise spectrum compared with the EN55022 limit Class B.

To provide a clearer and more concise overview of the findings, Table 3 summarizes the key observations extracted from Figs 10 to 15. The table highlights the influence of duty cycle variation on both common-mode and differential-mode emissions, showing that increasing the duty cycle substantially reduces CM levels and moderately decreases DM noise. It also presents the comparative behavior of the MOSFET- and IGBT-based configurations, where the MOSFET consistently generates higher CM and DM emissions due to its faster switching characteristics. Furthermore, the table consolidates the compliance assessment with the EN55022 Class B standard, illustrating that CM emissions remain within acceptable limits over most of the spectrum, while DM emissions exceed the limits mainly in the lower-frequency

region. This consolidated view helps emphasize the dominant trends and facilitates a clearer interpretation of the converter's EMI behavior under varying operating and device conditions.

Table 3. Summary of EMI results.

Category	Key result	Detailed findings
Effect of Duty Cycle on CM Emissions	Higher duty cycle reduces CM noise	CM amplitude decreases significantly from 15% to 90% duty cycle across 10–30 MHz (up to ~66% reduction at some frequencies).
Effect of Duty Cycle on DM Emissions	Higher duty cycle slightly reduces DM noise	DM emissions drop moderately when duty cycle increases (≈5–10 dBµV reduction depending on frequency). Fundamental switching region (~150 kHz) shows ~8% amplitude difference.
Comparison of Switching Devices – CM	MOSFET produces higher CM noise than IGBT	At 1 MHz: MOSFET ≈ 66 dBµV vs IGBT ≈ 57 dBµV. At high frequencies (~10 MHz), MOSFET remains ~10% noisier.
Comparison of Switching Devices – DM	MOSFET produces slightly higher DM noise	At 150 kHz: MOSFET ≈ 74 dBµV vs IGBT ≈ 68 dBµV. High-frequency DM differences remain smaller but still present.
CM Compliance with EN55022 Class B	CM passes Class B except at very low frequencies	Exceeds Class B between 0.15–0.75 MHz but fully compliant from 0.75–30 MHz.
DM Compliance with EN55022 Class B	DM fails Class B at low frequencies	DM emissions exceed Class B limits between 0.15–2.5 MHz but meet the limits for 2.5–30 MHz.

4. CONCLUSION

This research focused on the EMI behavior of a series chopper converter to validate its compliance with the EN55022 Class B standard. The study found that common-mode emissions were effectively managed in most situations; however, in the low-frequency range, differential-mode noise predominated and required further mitigation. Additionally, it was observed that IGBT devices were quieter than MOSFETs in terms of common-mode emissions, making them more suitable for high-power converter applications where EMI compliance is a critical concern.

From a design perspective, it is possible to manage EMI without compromising converter efficiency by employing differential-mode filtering, optimizing the duty cycle, and tuning gate resistance. Future investigations will focus on developing predictive EMI models that rely on control parameters, which will support the initial phase of EMC design and optimization. The insights gained from this research provide practical guidelines to reduce EMI while ensuring necessary approvals. Ultimately, this work will contribute to improving the reliability and efficiency of power electronic systems.

Acknowledgement : This research was supported by «La Direction Générale de la Recherche Scientifique et du Développement Technologique (DGRSDT)».

REFERENCES

[1] Z. Abdelkarim, N. Chikhi, "Experimental measurement of common and differential modes for variable speed drive DC motor," 19th International Multi-Confernce on Systems, Signals & Devices, 2022, doi: 10.1109/SSD54932.2022.9955933.

[2] S. Nemmich, M. Oukli, "Characterization of conducted electromagnetic interference (EMI) generated by switch mode power supply (SMPS)," Proceedings of ICEE, Batna, 2012.

[3] S. Ardjoun, A. Nour, I. Mahariq, "Experimental investigation of conducted electromagnetic interference differential-mode performance in various split-phase induction motors designs," *Results in Engineering*, vol. 17, 2025, pp.103–117. doi: 10.1016/j.rineng.2025.103963.

[4] A. Dahak, "Optimization of EMC filter for a variable speed drive system in electric aircraft," The Eurasia Proceedings of Science Technology Engineering and Mathematics, 2023, pp. 60-66, doi: 10.55549/epstem.1409311

[5] S. Bechkir, S. Hallima, "Effectiveness of shielding on the magnetic emissions emitted by a toroidal inductor," 2nd International Conference on Advanced Electrical Engineering, 2022, doi: 10.1109/ICAEE53772.2022.9962063.

[6] A. Gourbi, "An investigation and analysis of a hybrid photovoltaic system for power supply," *Ingeniería Energética Journal*, vol. 43, no. 3, pp. 1–11, 2022.

[7] L. Elamine, M. Hamza, "Comparative research in common and differential modes of EMI propensity in series and parallel chopper drives for DC motors," *Przegląd Elektrotechniczny*, vol. 7, pp. 151-157, 2025, doi: 10.15199/48.2025.07.24.

[8] N. Miloudi, A. Bendaoud, "Characterizing radiated electromagnetic interference from a power converter for improved electromagnetic compatibility," *WSEAS Transactions on Circuits and Systems*, vol. 23, pp. 135-148, 2025. doi: 10.37394/23201.2025.24.16.

[9] A. Gourbi, M. Miloudi, "Comparative analysis of differential-mode impedance in single-phase induction motors," *WSEAS Transactions on Circuits and Systems*, vol. 23, pp. 261-273, 2024. doi: 10.37394/23201.2024.23.26.

[10] A. Singh, K. Bharti, and N. Kumar, "Comparative study between DC-DC buck converter and Zero Voltage switching buck converter," in 2024 IEEE International Students' Conference on Electrical, Electronics and Computer Science (SCEECS), Bhopal, India: IEEE, Feb. 2024, pp. 1–6. doi: 10.1109/SCEECS61402.2024.10482318.

[11] Y. Lee, D. Kim, J. Kim, "A GaN driver IC with a TDC-based dead-time controller For GaN DC-DC buck converters," 20th International SoC Design Conference, 2023, doi: 10.1109/ISOCC59558.2023.10396085.

[12] S. Wu, Z. Ran, Z. Tong, T. Liu, Y. Lu, "A monolithic integrated e-mode GaN 48V-to-1V DC-DC buck converter with PWM control," IEEE International Conference on Integrated Circuits, Technologies and Applications, 2023, doi: 10.1109/ICTA60488.2023.10364290.

[13] H. Miloudi, M. Miloudi, "A high-frequency modeling of AC motor in a frequency range from 40 Hz to 110 MHz," *Electrical Engineering & Electromechanics*, vol. 6, pp.3–7, 2022, doi: 10.20998/2074-272X.2022.6.01.

[14] M. Lahlaci, "Experimental electromagnetic compatibility of conducted electromagnetic interferences from an IGBT and a MOSFET in the power supply," *Electrical Engineering & Electromechanics*, no. 3, pp. 38–43, 2024, doi: 10.20998/2074-272X.2024.3.05.

[15] Z. Ma, S. Wang, "Prediction and measurement techniques for radiated EMI of power converters with cables," *Chinese Journal of Electrical Engineering*, vol. 8, no. 4, pp. 1–10, Dec. 2022, doi: 10.23919/CJEE.2022.000033.

[16] D. Muller, D. Schweitzer, M. Beltle, S. Tenbohlen, "An active common mode EMI filter approach introducing predictive pulsed compensation," International Symposium on Electromagnetic Compatibility - EMC EUROPE, Barcelona, 2019, doi: 10.1109/EMCEurope.2019.8872104.

[17] F. Kharanaq, A. Emadi, B. Bilgin, "Modeling of conducted emissions for EMI analysis of power converters: state-of-the-art review," IEEE Access, vol. 8, pp. 189313–189325, 2020, doi: 10.1109/ACCESS.2020.3031693.

[18] S. Xu, Y. Peng, S. Li, "Suppression effectiveness research on multi-level EMI filter in thermal electromagnetic interactive filed of explosion-proof three-level NPC converter," *Case Studies in Thermal Engineering*, vol. 15, p. 100510, 2019, doi: 10.1016/j.csite.2019.100510.

[19] Z. Zhang, Y. Hu, X. Chen, G. Jewell, H. Li, "A review on conductive common-mode EMI suppression methods in inverter fed motor drives," *IEEE Access*, vol. 9, pp. 18345–18360, 2021, doi: 10.1109/ACCESS.2021.3054514.

[20] Y. Li, H. Zhang, S. Wang, H. Sheng, C. Chng, S. Lakshmikanthan, "Investigating switching transformers for common mode EMI reduction to remove common mode EMI filters and Y-capacitors in flyback converters," *IEEE Journal of Emerging and Selected Topics in Power Electronics*, vol. 6, no. 4, pp. 2287–2301, 2018, doi: 10.1109/JESTPE.2018.2827041.

[21] B. Hamza, G. Aek, "High-frequency Differential Mode Modeling of Universal Motor's Windings," *International Journal of Electrical and Electronics Research*, vol. 11, no. 4, pp. 1057–1064, 2023, doi: 10.37391/ijeer.110425.

[22] Y. Hakmi, "Frequency experimental identification approach for single-phase induction motor common-mode parameters," *Electrical Engineering & Electromechanics*, vol. 6, pp. 3–10, 2025, doi: 10.20998/2074-272X.2024.6.01.

[23] S. Takahashi, K. Wada, H. Ayano, S. Ogasawara, T. Shimizu, "Review of modeling and suppression techniques for electromagnetic interference in power conversion systems," *Journal of Industry Applications*, vol. 11, no. 1, pp. 2–14, 2022. doi: 10.1541/ieejjia.21006800.

[24] L. Yuan, J. Zhang, Z. Liang, M. Hu, G. Chen, W. Lu, W, "EMI challenges in modern power electronic-based converters: Recent advances and mitigation techniques," *Frontiers in Electronics*, vol. 4, 2023, https://doi.org/10.3389/felec.2023.1274258.

[25] N. Kojima, T. Hattori, W. Kitagawa, T. Takeshita, "Modeling method for conducted noise from power converter for power line communication", 11th International Conference on Power Electronics and ECCE Asia, 2023, doi: 10.23919/ICPE2023-ECCEAsia54778.2023.10213636.

[26] A. Zulfikaroglu, A. Gursel, "Ripple and passive components reduction on All SiC multi-device interleaved boost converter for hybrid electric vehicles," *Jordan Journal of Electrical Engineering*, vol. 9, no. 4, pp. 607–617, 2023. doi: 10.5455/jjee.204-1680506910.

[27] M. Tanashu, T. Tadiwos, A. Kassaw, "Multi-objective optimization of SEPIC-Cuk converter for photovoltaic application," *Jordan Journal of Electrical Engineering*, vol. 11, no. 1, pp. 151–167, 2025, doi: 10.5455/jjee.204-1722004077.

[28] B. Zhang, S. Wang, "A survey of EMI research in power electronics systems with wide-bandgap semiconductor devices," *IEEE Journal of Emerging and Selected Topics in Power Electronics*, vol. 8, no. 1, pp. 626–643, 2020, doi: 10.1109/JESTPE.2019.2953730.

[29] M. Houcine, B. Abdelber, M. Mohamed, "Réduction des perturbations électromagnétiques conduites dans la machine asynchrone," *Mediterranean Journal of Modeling and Simulation*, vol. 2, no. 1, pp.8-15, 2014.

[30] A. Tilmatine, L. Canale, "Experimental measurement of harmonic distortion and electromagnetic interferences for LED lamps," IEEE Industry Applications Society Annual Meeting, 2022, doi: 10.1109/IAS54023.2022.9940136

[31] L. Zhai, T. Zhang, Y. Cao, S. Yang, S. Kavuma, H. Feng, "Conducted EMI prediction and mitigation strategy based on transfer function for a high-low voltage DC-DC converter in electric vehicle," *Energies*, vol. 11, no. 5, p. 1028, 2018, doi: 10.3390/en11051028.

[32] M. Salhi, A. Al–Omari, "Experimental characterization of the high–frequency isolating power transformer," *Journal of Electrical Engineering and Computer Science*, vol. 86, no. 4, pp. 211–218, 2019.

[33] A. Gourbi, H. Slimani, "Common mode conducted electromagnetic interference in inverter – fed – AC – motor," *Electrical and Electronics Engineers Review*, pp.271–275, 2010.

[34] M. Laour, R. Tahmi, C. Vollaire, "Modeling and analysis of conducted and radiated emissions due to common mode current of a buck converter," *IEEE Transactions on Electromagnetic Compatibility*, vol. 59, no. 4, pp. 1260–1267, Aug. 2017, doi: 10.1109/TEMC.2017.2651984.

[35] A. Zeghoudi, H. Slimani, L. Canale, "Experimental measurements of near magnetic field by different probe for AC/DC LED driver," IEEE International Conference on Environment and Electrical Engineering, 2022, doi: 10.1109/EEEIC/ICPSEurope54979.2022.9854788.

[36] J. Yao, S. Wang, Z. Luo, "Modeling, analysis, and reduction of radiated emi due to the voltage across input and output cables in an automotive non-isolated power converter," *IEEE Transactions on Power Electronics*, vol. 37, no. 5, pp. 5455–5465, 2022, doi: 10.1109/TPEL.2021.3128628.

[37] S. Ghalem, A. Bendaoud, "Prediction of conducted disturbances generated by a DC/DC converter," *Eurasia Proceedings of Science, Technology, Engineering & Mathematics*, vol. 26, pp. 507–518, 2023, doi: 10.55549/epstem.1411082.